



## Analysis of the modulation in the first harmonic of the right ascension distribution of cosmic rays detected at the Pierre Auger Observatory

HARIS LYBERIS<sup>1,2</sup>, FOR THE PIERRE AUGER COLLABORATION<sup>3</sup>

<sup>1</sup>IPN Orsay, CNRS/IN2P3 & Université Paris Sud, Orsay, France

<sup>2</sup>Università degli Studi di Torino, Torino, Italy

<sup>3</sup> Observatorio Pierre Auger, Av. San Martín Norte 304, 5613 Malargüe, Argentina

(Full author list: [http://www.auger.org/archive/authors\\_2011\\_05.html](http://www.auger.org/archive/authors_2011_05.html))

[auger\\_spokespersons@fnal.gov](mailto:auger_spokespersons@fnal.gov)

**Abstract:** We present an update of the results of searches for first harmonic modulations in the right ascension distribution of cosmic rays detected with the surface detector of the Pierre Auger Observatory over a range of energies. The upper limits obtained provide the most stringent bounds at present above  $2.5 \times 10^{17}$  eV. The infill surface detector array which is now operating at the Pierre Auger Observatory will allow us to extend this search for large scale anisotropies to lower energy thresholds.

**Keywords:** Ultra-high energy cosmic rays, large scale anisotropies, Pierre Auger Observatory.

## 1 Introduction

The large scale distribution of arrival directions of cosmic rays represents one of the main tools for understanding their origin, in particular in the EeV energy range - where  $1 \text{ EeV} \equiv 10^{18} \text{ eV}$ . Using the large statistics provided by the surface detector (SD) array of the Pierre Auger Observatory, upper limits below 2% at 99% *C.L.* have been recently reported [1] for EeV energies on the dipole component in the equatorial plane. Such upper limits are sensible, because cosmic rays of galactic origin, while escaping from the galaxy in this energy range, might generate a dipolar large-scale anisotropy with an amplitude at the % level as seen from the Earth [2, 3]. Even for isotropic extragalactic cosmic rays, a large scale anisotropy may be left due to the motion of our galaxy with respect to the frame of extragalactic isotropy. This anisotropy would be dipolar in a similar way to the *Compton-Getting effect* [4] in the absence of the galactic magnetic field, but this field could transform it into a complicated pattern as seen from the Earth, described by higher order multipoles [5].

Continued scrutiny of the large scale distribution of arrival directions of cosmic rays as a function of the energy is thus important to constrain different models for the cosmic rays origin. To do so, we present an update of the results of searches for anisotropies by applying first harmonic analyses to events recorded by the SD array data from 1 January 2004 to 31 December 2010, with the same criteria for event selection as in [1].

## 2 First harmonic analyses

### 2.1 Analysis methods

A dipolar modulation of *experimental origin* in the distribution of arrival times of the events with a period equal to one solar day may induce a spurious anisotropy in the right ascension distribution. Such spurious variations can be accounted for thanks to the monitoring of the number of unitary cells  $n_{\text{cell}}(t)$  recorded every second by the trigger system of the Observatory, reflecting the array growth as well as the dead periods of each surface detector. Here, accordingly to the fiducial cut applied to select events [6], a unitary cell is defined as an active detector surrounded by six neighbouring active detectors. For any periodicity  $T$ , the total number of unitary cells  $N_{\text{cell}}(t)$  as a function of time  $t$  within a period and summed over all periods, and its associated relative variations are obtained from :

$$N_{\text{cell}}(t) = \sum_j n_{\text{cell}}(t + jT), \quad \Delta N_{\text{cell}}(t) = \frac{N_{\text{cell}}(t)}{\langle N_{\text{cell}}(t) \rangle}. \quad (1)$$

with  $\langle N_{\text{cell}}(t) \rangle = 1/T \int_0^T dt N_{\text{cell}}(t)$ . Hence, to perform a first harmonic analysis accounting for the slightly non-uniform exposure in different parts of the sky, we weight each event with right ascension  $\alpha_i$  by the inverse of the integrated number of unitary cells for computing the Fourier coefficients  $a$  and  $b$  :

$$a = \frac{2}{\mathcal{N}} \sum_{i=1}^{\mathcal{N}} \frac{\cos(\alpha_i)}{\Delta N_{\text{cell}}(\alpha_i^0)}, \quad b = \frac{2}{\mathcal{N}} \sum_{i=1}^{\mathcal{N}} \frac{\sin(\alpha_i)}{\Delta N_{\text{cell}}(\alpha_i^0)}, \quad (2)$$

29

30

31

32

33

34

35

36

37

38

39

40

41

42

43

44

45

46

47

48

49

50

51 where  $\mathcal{N} = \sum_{i=1}^N [\Delta N_{\text{cell}}(\alpha_i^0)]^{-1}$  and  $\alpha_i^0$  is the local side-  
 52 real time expressed here in radians and chosen so that it  
 53 is always equal to the right ascension of the zenith at the  
 54 center of the array. The amplitude  $r$  and phase  $\varphi$  are then  
 55 given by  $r = \sqrt{a^2 + b^2}$  and  $\varphi = \arctan(b/a)$ , and fol-  
 56 low respectively a Rayleigh and uniform distributions in  
 57 the case of an underlying isotropy.

58 Changes in the air density and pressure have been shown  
 59 to affect the development of extensive air showers and con-  
 60 sequently to induce a temporal variation of the observed  
 61 shower size at a fixed energy [7]. Such an effect is im-  
 62 portant to control, because any seasonal variation of the  
 63 modulation of the daily counting rate induces sidebands at  
 64 both the sidereal and the anti-sidereal frequencies, which  
 65 may lead to misleading measures of anisotropy in case the  
 66 amplitude of the sidebands significantly stands out from  
 67 the background noise [8]. To eliminate these variations,  
 68 the conversion of the shower size into energy is performed  
 69 by relating the observed shower size to the one that would  
 70 have been measured at reference atmospheric conditions.  
 71 Above 1 EeV, this procedure is sufficient to control the size  
 72 of the sideband amplitude to well below  $\simeq 10^{-3}$  [1].

73 Below 1 EeV, as weather effects affect the detection effi-  
 74 ciency to a larger extent, spurious variations of the count-  
 75 ing rate are amplified. Hence, we adopt the differential  
 76 *East-West method* [9]. Since the instantaneous exposure for  
 77 Eastward and Westward events is the same, the difference  
 78 between the event counting rate measured from the East  
 79 sector,  $I_E(\alpha^0)$ , and the West sector,  $I_W(\alpha^0)$ , allows us to  
 80 remove at first order the direction independent effects of ex-  
 81 perimental origin without applying any correction, though  
 82 at the cost of a reduced sensitivity. This counting differ-  
 83 ence is directly related to the right ascension modulation  $r$   
 84 by [9]:

$$I_E(\alpha^0) - I_W(\alpha^0) = -\frac{N}{2\pi} \frac{2 \langle \sin(\theta) \rangle}{\pi \langle \cos(\delta) \rangle} r \sin(\alpha^0 - \varphi). \quad (3)$$

85 where  $\delta$  is the declination and  $\theta$  the zenith angle of the de-  
 86 tected events. The amplitude  $r$  and phase  $\varphi$  can thus be cal-  
 87 culated from the arrival times of  $N$  events using the stan-  
 88 dard first harmonic analysis slightly modified to account  
 89 for the subtraction of the Western sector to the Eastern one.  
 90 The Fourier coefficients  $a_{EW}$  and  $b_{EW}$  are thus defined  
 91 by:

$$\begin{aligned} a_{EW} &= \frac{2}{N} \sum_{i=1}^N \cos(\alpha_i^0 + \zeta_i), \\ b_{EW} &= \frac{2}{N} \sum_{i=1}^N \sin(\alpha_i^0 + \zeta_i), \end{aligned} \quad (4)$$

92 where  $\zeta_i$  equals 0 if the event is coming from the East  
 93 or  $\pi$  if coming from the West (so as to effectively sub-  
 94 tract the events from the West direction). This allows us  
 95 to recover the right ascension amplitude  $r$  and the phase  
 96  $\varphi_{EW}$  from  $r = \frac{\pi \langle \cos(\delta) \rangle}{2 \langle \sin(\theta) \rangle} \sqrt{a_{EW}^2 + b_{EW}^2}$  and  $\varphi_{EW} =$   
 97  $\arctan(b_{EW}/a_{EW})$ . Note however that  $\varphi_{EW}$ , being the

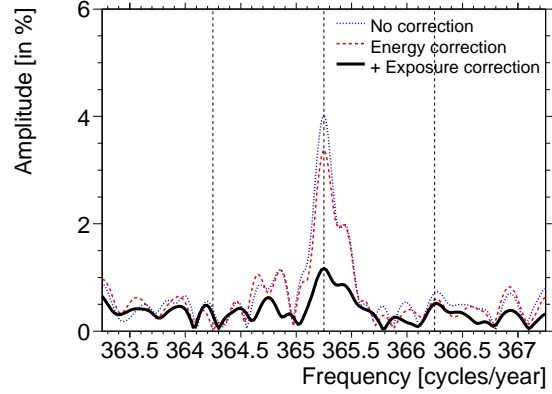


Figure 1: Amplitude of the Fourier modes as a function of the frequency above 1 EeV (see text).

phase corresponding to the maximum in the differential  
 of the East and West fluxes, is related to  $\varphi$  through  $\varphi =$   
 $\varphi_{EW} + \pi/2$ .

## 2.2 Analysis of solar frequency above 1 EeV

Over a 7-years period, spurious modulations are partially  
 compensated in sidereal time. Though, since the ampli-  
 tude of an eventual sideband effect is *proportional* to the  
 solar amplitude, it is interesting to look at the impact of  
 the corrections at and around the solar frequency by per-  
 forming the Fourier transform of the modified time distri-  
 bution [10]:

$$\tilde{\alpha}_i^0 = \frac{2\pi}{T_{sid}} t_i + \alpha_i - \alpha_i^0. \quad (5)$$

The amplitude of the Fourier modes when considering all  
 events above 1 EeV are shown in Fig. 1 as a function of fre-  
 quencies close to the solar one (dashed line at 365.25 cy-  
 cles/year). The thin dotted curve is obtained without ac-  
 counting for the variations of the exposure and without ac-  
 counting for the weather effects. There is a net solar ampli-  
 tude of  $\sim 4\%$ , highly significant. The impact of the cor-  
 rection of the energies is evidenced by the dashed curve  
 within the resolved solar peak (reduction of  $\simeq 20\%$  of the  
 spurious modulations). In addition, when accounting also  
 for the exposure variation at each frequency, the solar peak  
 is then reduced at a level close to the statistical noise, as  
 evidenced by the thick curve. This provides support that  
 the variations in the exposure and weather effects are under  
 control.

## 2.3 Analysis of the sidereal frequency

The amplitude  $r$  at the sidereal frequency as a function of  
 the energy is shown in Fig. 2. The size of the energy in-  
 tervals was chosen to be  $\Delta \log_{10}(E) = 0.3$  below 8 EeV,  
 so that it was larger than the energy resolution (about 15%  
 [11]) even at low energies. Above 8 EeV, to guarantee the

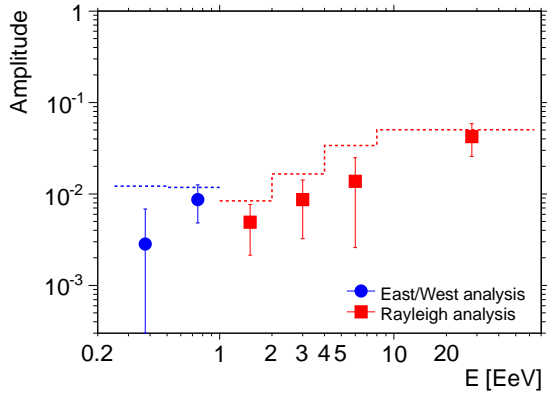


Figure 2: Amplitude of the first harmonic as a function of energy. The dashed line indicates the 99% *C.L.* upper bound on the amplitudes that could result from fluctuations of an isotropic distribution.

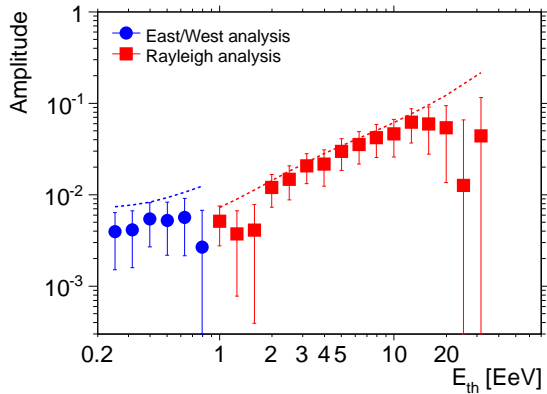


Figure 3: Same as Fig. 2, but as a function of energy thresholds.

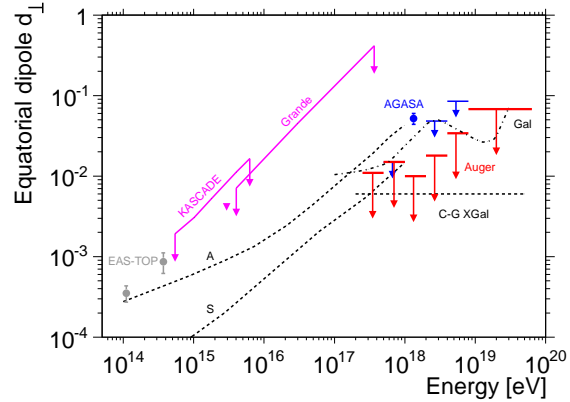


Figure 4: Upper limits on the anisotropy : equatorial dipole component  $d_{\perp}$  as a function of energy from this analysis. Results from EAS-TOP, AGASA, KASCADE and KASCADE-Grande experiments are also displayed, in addition to several predictions (see text).

### 3 Upper limits

144

From the analyses reported in the previous Section, upper limits on amplitudes at 99% *C.L.* can be derived according to the distribution drawn from a population characterised by an anisotropy of unknown amplitude and phase as derived by Linsley [12]. The Rayleigh amplitude measured by an observatory depends on its latitude and on the range of zenith angles considered. The measured amplitude can be related to a real equatorial dipole component  $d_{\perp}$  by  $d_{\perp} \simeq r / \langle \cos \delta \rangle$ , where  $\delta$  is the declination of the detected events, allowing a direct comparison of results from different experiments and from model predictions [1]. The upper limits on  $d_{\perp}$  are shown in Fig. 4, together with previous results from EAS-TOP [13], KASCADE [14], KASCADE-Grande [15] and AGASA [16], and with some predictions for the anisotropies arising from models of both galactic and extragalactic cosmic ray origin. In models *A* and *S* (*A* and *S* standing for 2 different galactic magnetic field symmetries) [3], the anisotropy is caused by drift motions due to the regular component of the galactic magnetic field, while in model *Gal* [17], the anisotropy is caused by purely diffusive motions due to the turbulent component of the field. Some of these amplitudes are challenged by our current sensitivity. For extragalactic cosmic rays considered in model *C-G Xgal* [18], the motion of our galaxy with respect to the CMB (supposed to be the frame of extragalactic isotropy) induces the small dipolar anisotropy (neglecting the effect of the galactic magnetic field).

145  
146  
147  
148  
149  
150  
151  
152  
153  
154  
155  
156  
157  
158  
159  
160  
161  
162  
163  
164  
165  
166  
167  
168  
169  
170  
171

### 4 Phase of first harmonic analyses

172

The phase of the first harmonic is shown in Fig. 5 as a function of the energy. While the measurements of the amplitudes do not provide any evidence for anisotropy, it does

173  
174  
175

130 determination of the amplitude measurement within an un-  
131 certainty  $\sigma \simeq 2\%$ , all events ( $\simeq 5,000$ ) were gathered in  
132 a single energy interval. The dashed line indicates the 99%  
133 *C.L.* upper bound on the amplitudes that could result from  
134 fluctuations of an isotropic distribution. There is no evi-  
135 dence of any significant signal in any energy range. The  
136 probability with which the 6 observed amplitudes could  
137 have arisen from an underlying isotropic distribution can be  
138 made by combining the amplitudes in all bins. It is found  
139 to be 45%.

140 Results of the analysis performed in terms of energy thresh-  
141 olds (strongly correlated bins) are shown in Fig. 3. They  
142 provide no further evidence in favor of a significant ampli-  
143 tude.

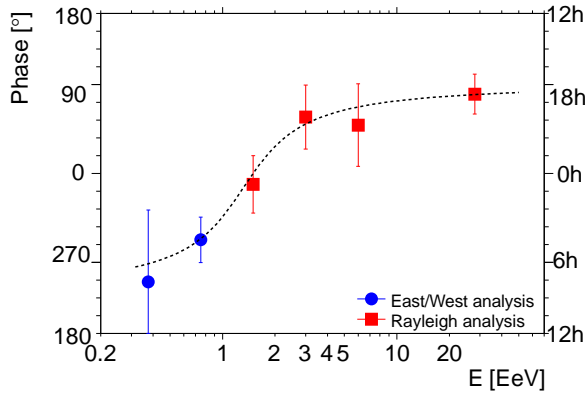


Figure 5: Phase of the first harmonic as a function of energy. The dashed line, resulting from an empirical fit, is used in the likelihood ratio test (see text).

176 not escape our notice that these measurements suggest a  
 177 smooth transition between a common phase of  $\simeq 270^\circ$  be-  
 178 low 1 EeV and another phase (right ascension  $\simeq 100^\circ$ )  
 179 above 5 EeV. This is potentially interesting, because with a  
 180 real underlying anisotropy, a consistency of the phase mea-  
 181 surements in ordered energy intervals is indeed expected  
 182 with lower statistics than that required for the amplitudes  
 183 to significantly stand out of the background noise [19]. To  
 184 quantify whether or not a parent random distribution of ar-  
 185 rival directions reproduces the phase measurements in adja-  
 186 cent energy intervals better than an alternative dipolar par-  
 187 ent distribution, we introduced a likelihood ratio test in our  
 188 previous report [1]. When applied to data points of Fig. 5,  
 189 this test leads to a probability of  $\sim 10^{-3}$  to accept the ran-  
 190 dom distribution compared to the alternative one. Since we  
 191 did not perform an *a priori* search for such a smooth tran-  
 192 sition in the phase measurements, no confidence level can  
 193 be derived from this result. With an independent data set  
 194 of comparable size, we will be able to confirm whether this  
 195 effect is real or not.

196 It is important to note that an apparent constancy of phase,  
 197 even though the significances of the amplitudes are rela-  
 198 tively small, has been pointed out previously in sur-  
 199 veys of measurements made in the range  $10^{14} < E <$   
 200  $10^{17}$  eV [20]. A clear tendency for maxima to occur around  
 201 20 hours l.s.t. was stressed, not far from our own measure-  
 202 ments in the energy range  $2.5 \times 10^{17} < E < 10^{18}$  eV.  
 203 Greisen *et al.* pointed out that most of these experiments  
 204 were conducted at northern latitudes, and therefore re-  
 205 garded the reality of such sidereal waves as not yet estab-  
 206 lished due to possible atmospheric effects leading to spuri-  
 207 ous waves. It is important that the Auger measurements are  
 208 made with events coming largely from the southern hemi-  
 209 sphere. In future analyses, we will benefit from the lower  
 210 energy threshold now available at the Pierre Auger Obser-  
 211 vatory thanks to the infill array [21], allowing a better over-  
 212 lap with the energy ranges presented in Ref. [20]. Prelimi-

nary analyses of this data with the East-West method show  
 also an apparent constancy of the phase.

## References

- [1] The Pierre Auger Collaboration, *Astropart. Phys.*, 2011, **34**: 627.
- [2] V. Ptuskin *et al.*, *Astron. Astrophys.*, 1993, **268**: 726.
- [3] J. Candia, S. Mollerach, E. Roulet, *JCAP*, 2003, **0305**: 003.
- [4] A.H. Compton, I.A. Getting, *Phys. Rev.*, 1935, **47**: 817.
- [5] D. Harari, S. Mollerach, E. Roulet, *JCAP*, 2010, **11**: 033.
- [6] The Pierre Auger Collaboration, *Nucl. Instr. Meth. A*, 2010, **613**: 29.
- [7] The Pierre Auger Collaboration, *Astropart. Phys.*, 2009, **32**: 89.
- [8] F.J.M.Farley and J.R.Storey, *Proc. Phys. Soc. A*, 1954, **67**: 996.
- [9] R. Bonino *et al.*, submitted to *ApJ*. See also H. Lyberis, paper 1145, these proceedings.
- [10] P. Billoir, A. Letessier-Selvon, *Astropart. Phys.*, 2008, **29**: 14.
- [11] R. Pesce, for the Pierre Auger Collaboration, paper 1160, these proceedings.
- [12] J. Linsley, *Phys. Rev. Lett.*, 1975, **34**: 1530.
- [13] The EAS-TOP Collaboration, *ApJ. Lett.*, 2009, **692**: 130.
- [14] The KASCADE Collaboration, *ApJ*, 2004, **604**: 687.
- [15] S. Over *et al.*, *Proc. 30th ICRC*, Merida, Mexico, 2007, **4**: 223.
- [16] N. Hayashida *et al.*, *Astropart. Phys.*, 1999, **10**: 303.
- [17] A. Calvez, A. Kusenko, S. Nagataki, *Phys. Rev. Lett.*, 2010, **105**: 091101.
- [18] M. Kachelriess, P. Serpico, *Phys. Lett. B*, 2006, **640**: 225.
- [19] J. Linsley and A.A. Watson, Private communications.
- [20] K. Greisen *et al.*, *Proc. International Conference on Cosmic Rays and Earth Storms*, Japan, 1962, *J. Phys. Soc. Japan* **17** (Suppl. A-III): 76.
- [21] M. Platino, for the Auger Collaboration, *Proc. 31st ICRC*, Lodz, Poland, 2009, arXiv:0906.2354[astro-ph].